Electron Spin Resonance and Electron Spin Echo Modulation Studies on the Formation and Adsorbate Interactions of Ni(I) in Synthetic Clinoptilolite

Hosun Choo, A. M. Prakash, Seung-Kyu Park, and Larry Kevan*

Department of Chemistry, University of Houston, Houston, Texas 77204-5641

Received: January 27, 1999; In Final Form: May 25, 1999

Electron spin resonance (ESR) and electron spin echo modulation (ESEM) spectroscopies were used to study the formation of Ni(I) by various reduction methods and various adsorbate interactions of Ni(I) in synthetic clinoptilolite, in which Ni(II) was ion-exchanged into extraframework sites of clinoptilolite. Thermal reduction by dehydration at 573 K shows a single species assigned to Ni(I) ions. Two isolated Ni(I) ions are observed after hydrogen reduction at 623 K. Adsorption of methanol on hydrogen-reduced NiNaK−Clino forms a Ni(I)−$(CD_3OH)_n$ complex resulting from the interaction of methanol with one of the isolated Ni(I) ions. Adsorption of ammonia on hydrogen-reduced NiNaK−Clino produces a prominent Ni(I)−$(ND_3)_n$ complex by interaction with both Ni(I) ions. The ^{13}C hyperfine structure and ESEM analysis parameters after ^{13}CO adsorption indicate that Ni(I) interacts with one CO molecule and forms a Ni(I)−$(CO)_1$ complex. Two Ni(I)−$(C_2D_4)_n$ complexes are generated after adsorption of ethylene on dehydrated Ni(II)NaK−Clino and subsequent heating below 623 K. At higher temperature, these species disappear with the concomitant formation of two Ni(I)−$(C_4D_8)_n$ complexes, indicating ethylene dimerization. ^2D ESEM confirms the coordination of Ni(I) with butene. Adsorption of NO on dehydrated Ni(II)NaK−Clino produces two Ni(I)−NO^+ complexes formed by transfer of the odd electron from NO to Ni(II) ions. Along with two Ni(I)−NO^+ species, another species assigned to the NO radical is also observed in NiNaK−Clino after NO adsorption on Ni(II)NaK−Clino and NaK−Clino.

Introduction

Clinoptilolite is a naturally occurring zeolite with an aluminum and silicon tetrahedral oxide framework, the crystal structure of which is composed of three channels denoted A, B, and C.[1,2] A 10-membered channel (A) and one eight-membered channel (B) run side by side along the *c*-axis. They are intersected by another eight-membered channel (C) that runs along the *a*-axis.[1] The chemical formula for clinoptilolite is $(Na,K)_6[Al_6Si_{30}O_{72}]\cdot 24H_2O$.[3] The negative charge of the clinoptilolite framework from tetrahedrally coordinated aluminum is balanced by Na and K. These cations can be exchanged to some extent by transition metal ions. Clinoptilolite has been investigated for gas purification and separation and for ion-exchange applications.[1,4]

The modification of clinoptilolite by incorporation of transition metal ions into ion-exchange sites is of potential significance for several catalytic reactions. Cu-exchanged zeolites have been used as catalysts for NO reduction.[5] Palladium-modified X and Y zeolites have exhibited catalytic activities for hydrogenation[6] and ethylene dimerization.[7,8] However, compared to X and Y zeolites, few studies have been done on clinoptilolite containing transition metals. This is mainly due to difficulties in the reliable synthesis of clinoptilolite due to the rather narrow ranges of Si/Al and OH/Si ratios of the gel necessary for the crystallization of this material.[9] Furthermore, impurities such as paramagnetic Fe(III) that are commonly found in natural samples limit the application of natural clinoptilolite as a catalyst as well as its characterization by electron spin resonance (ESR) and electron spin echo modulation (ESEM) spectroscopies. Recently, the conditions for reliable synthesis of Na,K−clinoptilolite have been established in our laboratory.[10]

Ni(I) ions stabilized in zeolite lattices are catalytically active sites for acetylene cyclomerization and ethylene oligomerization.[11,12] The catalytic properties of nickel-exchanged zeolites are strongly dependent on the nature and location of the Ni ions as well as on their accessibility and coordination with various adsorbates. In the past, ESR spectroscopy has been used effectively to characterize the oxidation states in nickel-exchanged zeolites. ESEM spectroscopy, when combined with ESR, has proved useful for determining the nickel ion locations and the number and orientation of adsorbates coordinating to Ni ions.

In this study, we investigated the formation of Ni(I) in synthetic clinoptilolite by various reduction methods and its interaction with adsorbates such as methanol, ammonia, and carbon monoxide. Incorporation of Ni(II) is achieved by ion exchange into extraframework sites. The formation of Ni(I) by thermal reduction and with H_2, CO, NO, and C_2H_4 has been investigated by ESR and ESEM spectroscopies.

Experimental Section

Synthesis. Single-phase Na,K−clinoptilolite was hydrothermally synthesized.[10] The following chemicals were used without further purification: 6 M NaOH solution, 6 M KOH solution, dried aluminum hydroxide, $Al(OH)_3$ (USP, Pfaltz & Bauer Inc.), colloidal silica (Ludox LS, Aldrich). Synthesis was carried out in small (10 mL) stainless steel autoclaves with Teflon liners at autogenous pressure. The addition of seed crystals was important to decrease the crystallization time. The molar composition of the reaction mixture was $0.29NaOH/1.33KOH/1Al(OH)_3/4.5SiO_2/54.2H_2O$. In a typical synthesis, 0.87 g of dried aluminum hydroxide was added to a mixture of 0.54 mL

10.1021/jp990324d CCC: $18.00
Published on Web 07/02/1999

of 6 M NaOH and 2.46 mL of 6 M KOH. After being stirred for 1 h, 8.26 mL of colloidal silica was added slowly and the mixture was further stirred for 1 h. Finally, 0.1 g of synthetic seed crystals of clinoptilolite was added to promote crystallization. The final mixture was put into a static autoclave and heated at 180 °C for 94 h. The final pH of the mother liquor was 9.6. After crystallization, the product was washed with water and dried at 70 °C overnight.

Synthesized Na,K−clinoptilolite was ion-exchanged with 1 N NaCl at 70 °C overnight. To ensure maximum exchange, this procedure was repeated three times. Ni(II) ions were introduced into clinoptilolite by ion-exchanging with 0.5 mM $NiCl_2 \cdot 6H_2O$ (Aldrich) solution at 60 °C for 24 h. The chemical composition of this sample was $Ni_{0.07}Na_{0.02}K_{0.02}[Al_{0.17}Si_{0.83}O_2]$ based on electron microprobe analysis. This final ion-exchanged sample is designated as NiNaK−Clino.

Sample Treatment and Measurement. Hydrated samples were loaded into 3 mm o.d. by 2 mm i.d. Suprasil quartz tubes that were evacuated overnight and sealed. To study the behavior of nickel as a function of hydration, the samples were slowly heated under vacuum ($<10^{-4}$ Torr) from 373 to 673 K at intervals of 100 K. This procedure accomplishes thermal reduction. ESR spectra were recorded at 77 K to detect the formation of any Ni(I) species. Reduction by molecular hydrogen was accomplished by evacuating at room temperature, gradual heating to 673 K for 24 h, contact with 500 Torr of dry O_2 at 623 K for 5 h, evacuation at 623 K, and thermal reduction in H_2 at 623 K for 1 h. During reduction in H_2 Ni(0) is easily formed, as indicated by a broad background signal in the ESR spectrum. Special care must be taken to avoid formation of metallic nickel by controlling the temperature, time, and hydrogen pressure. To investigate the formation of Ni(I) reduced by the interaction with ^{12}CO (Cambridge Isotopes), ^{13}CO (Cambridge Isotopes), NO (Linde), C_2D_4 (Cambridge Isotopes), and 1-butene (Linde), Ni(II)-exchanged clinoptilolite was treated by the above dehydration and oxidation procedures before being exposed to the reducing gas. To prepare Ni(I) complexes with various adsorbates, hydrogen-reduced samples were evacuated at room temperature for 10 min and then exposed to the room-temperature vapor pressure of CD_3OH (Stohler Isotope), 20 Torr of ND_3 (Cambridge Isotopes), 14 and 100 Torr of ^{13}CO, and 20 Torr of C_2D_4. These samples with adsorbates were frozen in liquid nitrogen and sealed for ESR and ESEM measurements.

ESR spectra were recorded with a Bruker ESP 300 X-band spectrometer at 77 K. The magnetic field was calibrated with a Varian E-500 gauss meter. The microwave frequency was measured by a Hewlett-Packard HP 5324A frequency counter. ESEM spectra were measured at 5 K with a Bruker ESP 380 pulsed ESR spectrometer. Three pulse echoes were measured by using a $\pi/2 - \tau - \pi/2 - T - \pi/2$ pulse sequence as a function of time T to obtain a time domain spectrum. ^{13}C modulation was obtained at a value of $\tau = 0.192$ μs, and deuterium modulation was obtained with $\tau = 0.256$ μs. The modulation was analyzed by a spherical approximation for powder samples in terms of N nuclei at distance R with an isotropic hyperfine coupling A_{iso}.[13] The best fit simulation of an ESEM signal is found by varying the parameters until the sum of the squared residuals is minimized.

Results

Thermal and Hydrogen Reduction of Nickel Ions in NiNaK−Clino. Hydrated NiNaK−Clino does not show any ESR signal at 77 K. Thus, the Ni ions exist in the form of Ni(II). Figure 1 shows the ESR spectra of thermally reduced NiNaK−Clino at 573 and 623 K. Dehydration of a sample below 573 K produces no paramagnetic species due to Ni(I) ions but a very sharp signal at $g = 1.998$. Dehydration at 573 K shows two paramagnetic species denoted A and B. Species A with $g_1^A = 2.296$, $g_2^A = 2.097$, and $g_3^A = 1.963$ can be assigned to Ni(I) ions formed by desorbing water and hydroxyl groups.[14] This rhombic species has not been reported previously in Ni(II)-exchanged X, Y zeolites and SAPO materials. Species B with $g = 1.998$ has been observed in several SAPO materials after dehydration and was tentatively assigned to a radical species.[15] Increasing the reduction temperature by only 50 K leads to the formation of a broad signal due to metallic nickel, suggesting that Ni(I) reduces to Ni(0) and that thermal reduction is highly sensitive to temperature (Figure 1b).

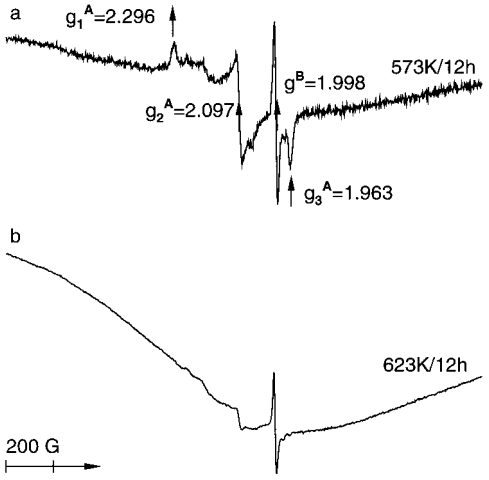

Figure 1. ESR spectra at 77 K of NiNaK−Clino (a) after dehydration at 573 K for 12 h and (b) after dehydration at 623 K for 12 h.

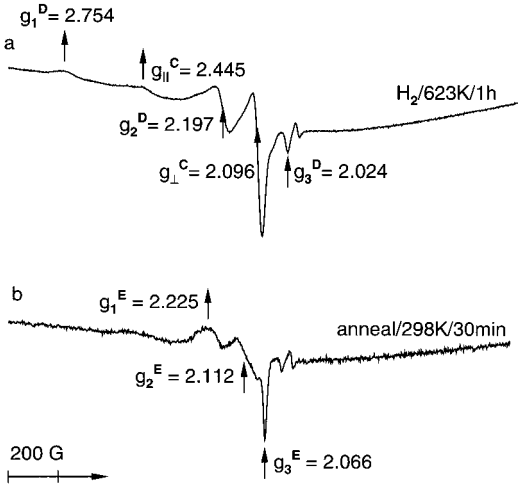

Figure 2. ESR spectra at 77 K of NiNaK−Clino (a) after H_2 treatment of a dehydrated sample at 623 K for 1 h and (b) after annealing of a H_2-treated sample at room temperature for 30 min.

Figure 2a shows the ESR spectra of NiNaK−Clino after hydrogen reduction at 623 K for 1 h. Two distinct Ni(I) species, denoted C and D, are observed. Species C has axial symmetry with $g_{||}^C = 2.445$ and $g_\perp^C = 2.096$. A species with g values similar to those of species C has been reported in SAPO-5,[16] SAPO-11,[14] and SAPO-41[17] and in Ni-exchanged zeolites[18,19] thermally or photochemically reduced in H_2 and was assigned to isolated Ni(I). Species D has $g_1^D = 2.754$, $g_2^D = 2.197$, and $g_3^D = 2.024$, indicating lower symmetry for this Ni(I). A rhombic species has been observed in NiCa−X zeolite[20] and was assigned to a $Ni-(H_2)_n$ species, since this species disappears

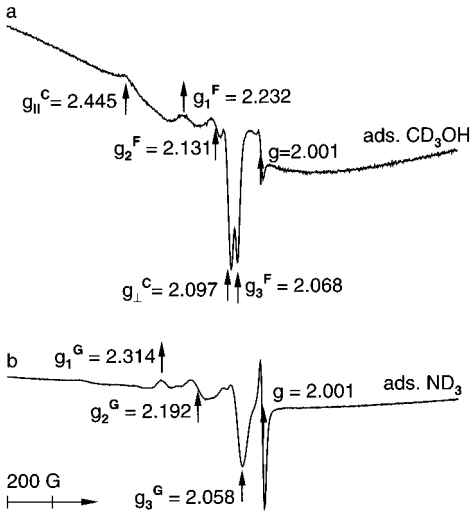

Figure 3. ESR spectra at 77 K of NiNaK−Clino (a) after CD_3OH adsorption on a hydrogen-reduced sample at room temperature for 2 min and (b) after ND_3 adsorption on a hydrogen-reduced sample at room temperature for 2 min.

upon evacuation of hydrogen at room temperature and reappears upon readsorption of hydrogen. However, the behavior of species D with respect to evacuation is different from that observed in NiCa−X zeolite. The intensities of species C and D decrease, but both species remain visible after a hydrogen-reduced sample is evacuated at room temperature. So, species D is also assigned to isolated Ni(I) ions in NiNaK−Clino.

A new species, designated as E, appears when a hydrogen-reduced sample is kept at room temperature in the presence of hydrogen (Figure 2b). Species E has rhombic symmetry with $g_1^{E} = 2.225$, $g_2^{E} = 2.112$, and $g_3^{E} = 2.066$.

Adsorbate Interactions. Figure 3a is the ESR spectrum after adsorption of methanol at room temperature on NiNaK−Clino. Hydrogen-reduced NiNaK−Clino shows both species C and D after evacuation of hydrogen at room temperature for 10 min. Exposure of this evacuated sample to CD_3OH causes species D to disappear completely, and simultaneously, a new species F appears with $g_1^{F} = 2.232$, $g_2^{F} = 2.131$, and $g_3^{F} = 2.068$ (Figure 3a). Species F retains the same intensity even after annealing at room temperature for 1 h. The facts that the ESR parameters of species F are different from those of a hydrogen-reduced sample and that species C remains almost unchanged after methanol adsorption support the hypothesis that species F results from the interaction of species D with methanol. This rhombic species has not been reported in previous X, Y zeolites or SAPO materials upon adsorption of methanol, indicating that this Ni(I) species in NiNaK−Clino is associated with the structure of NiNaK−Clino.

Adsorption of ND_3 at room temperature on NiNaK−Clino produces a single species G with rhombic symmetry and ESR parameters $g_1^{G} = 2.314$, $g_2^{G} = 2.192$, and $g_3^{G} = 2.058$ (Figure 3b). A rhombic species with similar ESR parameters has been observed in NiH−SAPO-41[15] where it was assigned to a Ni(I)−$(ND_3)_n$ species. It is interesting to note that unlike with methanol adsorption, species C and D both disappear almost completely with ammonia adsorption with the simultaneous formation of species G. This suggests that ammonia coordinates with both Ni(I) species C and D.

ESR spectra recorded after CO adsorption at room temperature for 2 min on hydrogen-reduced NiNaK−Clino are shown in Figure 4. When 100 Torr of CO is adsorbed, species H with $g_1^{H} = 2.253$, $g_2^{H} = 2.192$, and $g_3^{H} = 2.064$ (Figure 4a) is

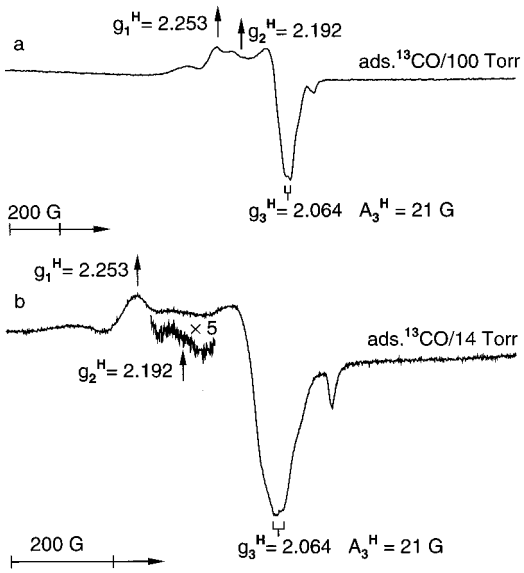

Figure 4. ESR spectra at 77 K of NiNaK−Clino (a) after 100 Torr of ^{13}CO adsorption and (b) after 14 Torr of ^{13}CO adsorption on a hydrogen-reduced sample at room temperature for 2 min.

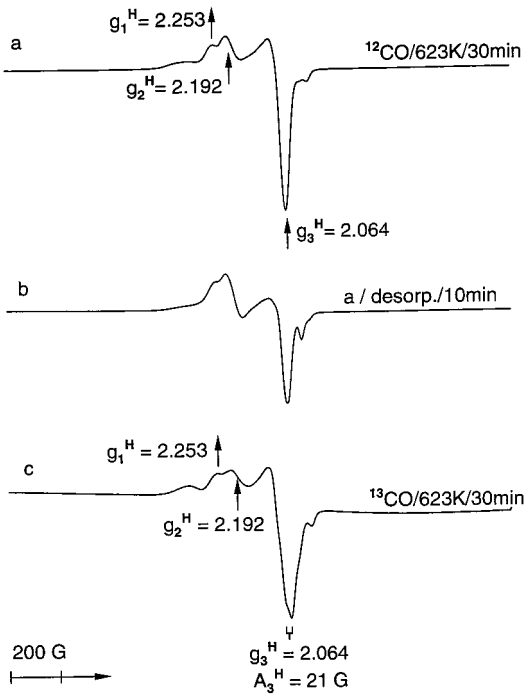

Figure 5. ESR spectra at 77 K of NiNaK−Clino (a) after adsorption of 20 Torr of ^{12}CO on dehydrated Ni(II)NaK−Clino at 623 K for 30 min, (b) after evacuation of a ^{12}CO-treated sample at room temperature for 10 min, and (c) after adsorption of 20 Torr of ^{13}CO on dehydrated Ni(II)NaK−Clino at 623 K for 30 min.

observed as a prominent species. From Figure 4b, it is clear that the ESR spectrum obtained after only 14 Torr of CO is exposed to Ni(I)NaK−Clino is almost the same as that observed upon adsorption of 100 Torr of CO. This behavior of Ni(I) toward CO indicates that the carbonyl complex of Ni(I) is not dependent on CO pressure in NiNaK−Clino. Species H can be directly obtained by reduction of dehydrated Ni(II)NaK−Clino by treatment with CO at 623 K for 30 min (Figure 5a,c). This prominent species H remains after evacuation of a CO-reduced sample (Figure 5b). It is also observed that the g_3 component of species G is split into two lines in the ESR spectrum when the sample is treated with 90% ^{13}C-enriched CO. This indicates

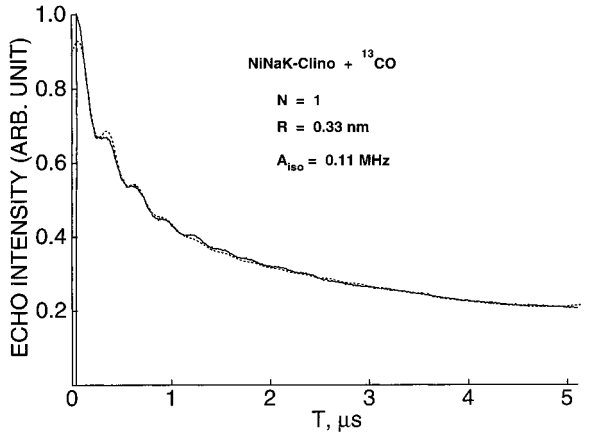

Figure 6. Experimental (−) and simulated (- - -) three-pulse ^{13}C ESEM spectra at 5 K of NiNaK−Clino after CO adsorption. The spectrum was recorded at a magnetic field corresponding to g_3 of species H.

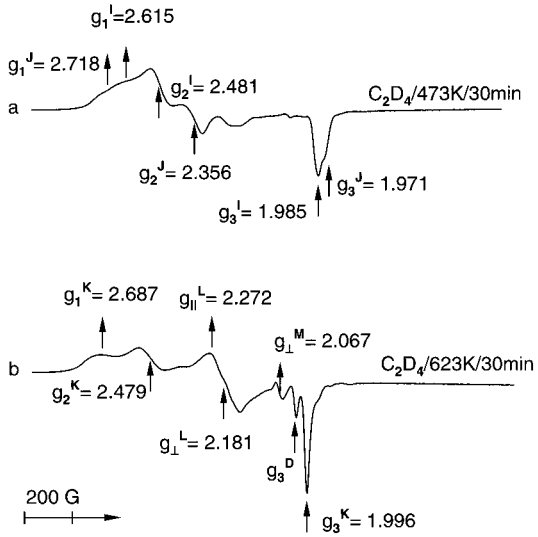

Figure 7. ESR spectra at 77 K of NiNaK−Clino after adsorption of 20 Torr of ethylene on hydrogen-reduced NiNaK−Clino at 298 K for 2 min and subsequently heated for 30 min at (a) 373 K and (b) 623 K.

that these Ni(I) ions interact with the nuclear spin of ^{13}C ($I = {}^1/_2$) of CO and lead to hyperfine splitting $A_3 = 21$ G. To determine the structure of the carbonyl complex with Ni(I), ^{13}C ESEM was carried out for NiNaK−Clino reduced with ^{13}CO. The experimental and simulated three-pulse ESEM spectra are shown in Figure 6. The best fit simulation indicates one carbon atom interacting with Ni(I) at 0.33 nm.

Ethylene adsorption at room temperature on hydrogen-reduced NiNaK−Clino produces a broad signal due to Ni(0) superimposed on signals assigned to Ni(I) species C and D. No signal due to a Ni(I)−C_2D_4 complex is observed. This indicates that ethylene reduces Ni(I) to Ni(0). Similar behavior has been reported for NiH−SAPO-41[17] where Ni(I) ions located in a 10-ring channel readily react with ethylene and are reduced to Ni(0). Figure 7 shows the ESR spectra of NiNaK−Clino after exposing dehydrated Ni(II)NaK−Clino to 20 Torr of ethylene at room temperature and then heating to various temperatures for 30 min. When a sample is heated to 473 K for 30 min (Figure 7a), two rhombic species, denoted I and J, are observed. Species I with $g_1^I = 2.615$, $g_2^I = 2.481$, and $g_3^I = 1.985$ has been reported in NiAPSO-5,[21] NiNa−Y,[12] and NiCa−X zeolite[20] and was assigned to a Ni(I)−$(C_2D_4)_n$ complex. Species J also has rhombic symmetry with ESR parameters $g_1^J = 2.718$, $g_2^J = 2.356$, and $g_3^J = 1.971$. Upon increasing the temperature from

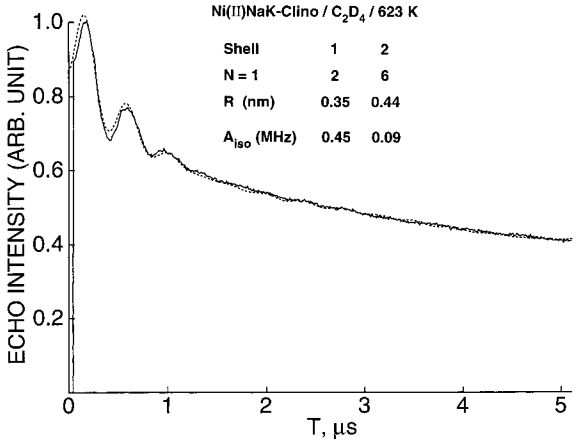

Figure 8. Experimental (−) and simulated (- - -) three-pulse ^{2}D ESEM spectra at 5 K after ethylene dimerization on NiNaK−Clino. The spectrum was recorded at a magnetic field corresponding to g_3 of species K.

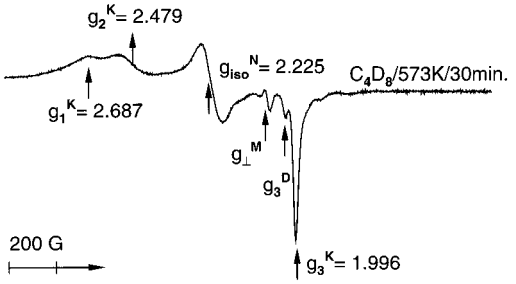

Figure 9. ESR spectra at 77 K of NiNaK−Clino after 1-butene treatment of dehydrated Ni(II)NaK−Clino at 573 K for 30 min.

473 to 573 K, the intensities of species I and J increase without any change of the ESR spectrum. These observations suggest that species I and J result from the reduction of Ni(II) to Ni(I) by ethylene and subsequent formation of a complex with ethylene. The ESR signals remain unchanged after prolonged heating of this sample at 473 K, indicating that no dimerization occurs in this system. Figure 7b shows that species I and J almost disappear with the formation of new species K and L when a sample is heated to 623 K for 30 min. Species K with $g_1^K = 2.687$, $g_2^K = 2.479$, and $g_3^K = 1.996$ is assigned to a Ni(I) complex with butene, which is a product of ethylene dimerization. This assignment is confirmed by ESEM data. Another species L with $g_{||}^L = 2.272$ and $g_\perp^L = 2.181$ probably arises from the interaction of Ni(I) with a product of ethylene dimerization, since this species appears at a higher temperature along with species K, a Ni(I)−$(C_4D_8)_n$ complex.

Figure 8 shows the experimental and simulated three-pulse deuterium ESEM spectra for species K obtained when 20 Torr of ethylene is exposed to hydrogen-reduced NiNaK−Clino at room temperature and the sample is heated to 623 K for 30 min. The magnetic field is set at the value corresponding to the g_3 component of species K. The best-fit simulation with a two-shell model shows two nearest-neighbor deuterium atoms at 0.35 nm and six next-nearest-neighbor deuterium atoms at 0.44 nm, indicating the formation of a Ni(I)−(C_4D_8) complex as a result of ethylene dimerization.

Figure 9 shows the ESR spectrum observed after 20 Torr of 1-butene is adsorbed on dehydrated Ni(II)NaK−Clino followed by heating to 573 K for 30 min. Two species, K and N, are observed. The g values of these species do not change for longer reaction time. Species K is the same as already observed after an ethylene-treated sample is heated at 623 K for 30 min.

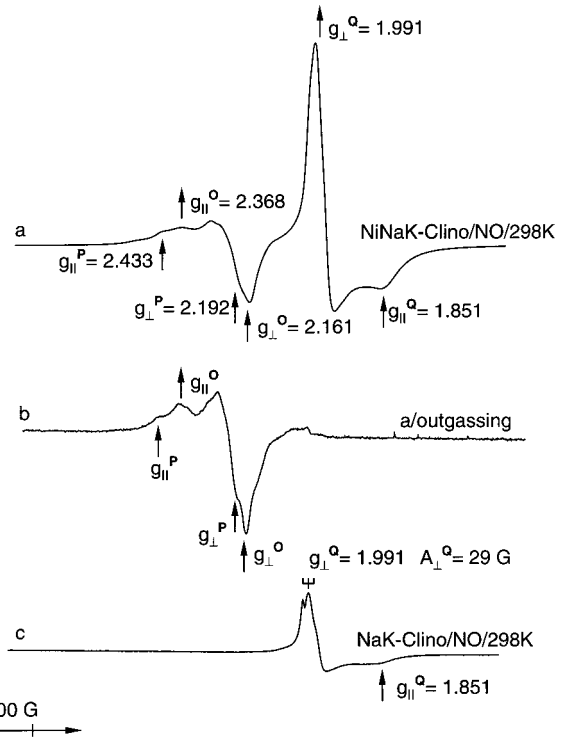

Figure 10. ESR spectra at 77 K (a) after 20 Torr of NO adsorption on dehydrated Ni(II)NaK−Clino at room temperature for 2 min, (b) after subsequent evacuation at room temperature for 10 min, and (c) after 2 Torr of NO adsorption on dehydrated NaK−Clino at room temperature for 2 min.

Species N has isotropic symmetry with $g_{iso}^N = 2.225$. This species has been observed in NiCa−Y zeolite[12] and in Ni(II)-exchanged SAPO-8 and was assigned to a Ni(I)−$(C_4D_8)_n$ complex.[22]

Figure 10a shows the ESR spectrum recorded at 77 K after adsorption of 20 Torr of NO at room temperature on dehydrated Ni(II)NaK−Clino for 2 min. This spectrum consists of three signals, species O, P, and Q. Both species O and P have axial g tensors $g_{||}^O = 2.368$, $g_\perp^O = 2.161$, $g_{||}^P = 2.433$, and $g_\perp^P = 2.192$ and remain after evacuation of NO at room temperature for 10 min (Figure 10b). The fact that species O and P are not observed when NO is adsorbed on NaK−Clino containing no Ni ions (Figure 10c) suggests that these species come from the interaction of Ni(I) with NO molecules. A third species, denoted as species Q, has axial symmetry with $g_{||}^Q = 1.851$ and $g_\perp^Q = 1.991$. This species is not observed when the spectrum is recorded at room temperature. The facts that the same species is observed when NO is adsorbed on NaK−Clino (Figure 10c) and that this species disappears upon evacuation of NO at room temperature lead to the assignment of species Q to NO molecules adsorbed on the lattice of clinoptilolite. The triplet feature of the perpendicular component $g_\perp^Q$ results from the hyperfine interaction with a ^{14}N nucleus ($I = 1$).

Table 1 summarizes the ESR parameters assigned to the various Ni(I) species observed in NiNaK−Clino and their assignments.

Discussion

Clinoptilolite is a channel-type zeolite that has a main 10-ring channel with an elliptical pore opening of 0.72 nm × 0.44 nm.[23] Four cation sites, M1−M4, have been determined in natural clinoptilolite using single-crystal X-ray diffraction.[3,24] The approximate positions of these sites are shown in Figure 11. The cations, at sites M1 and M2, coordinate with water molecules and four and three framework oxygens, respectively. During dehydration, cations in these sites migrate close to M3 sites and the distance between the cation and framework oxygen becomes shorter. These sites are typically occupied by sodium. Site M1 is the only cation site found in the main 10-ring channel after dehydration. The cations at M3 sites are coordinated to six framework oxygens and two water molecules at the center of channel C. This site is typically occupied by potassium. At M4 sites, the cation is not bonded to any framework oxygen but is fully coordinated with water molecules. These four sites are too close to one another to be occupied side by side at the same time.

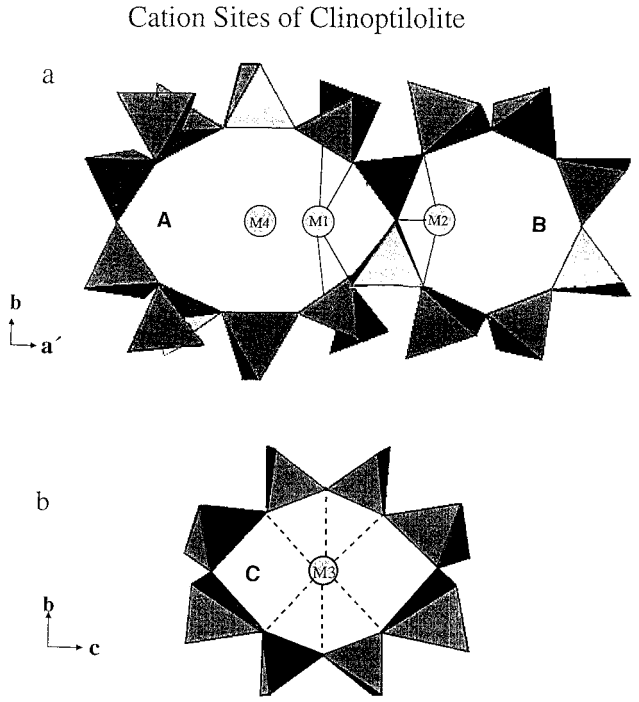

Figure 11. (a) View along the *c*-axis parallel to a 10-ring channel (A) and an 8-ring channel (B). (b) View along the *a*-axis parallel to an 8-ring channel (C). M1−M4 represent cation locations in the clinoptilolite structure. The corners of the tetrahedra represent framework oxygens. Al and Si atoms are located at the centers of the tetrahedra. Adapted from ref 24.

TABLE 1: ESR *g* Values of Ni(I) Species in NiNaK−Clino Produced during Various Reduction Methods and after Adsorbate Interactions

reduction method	adsorbate	assignment	$g_{\|\|}$ or g_1	$g_\perp$ or g_2	g_3	species
thermal	none	Ni(I)	2.296	2.097	1.963	A
H_2	none	Ni(I)	2.754	2.197	2.024	D
		Ni(I)	2.445	2.096		C
		Ni(I)−$(H)_n$	2.225	2.112	2.066	E
H_2	CD_3OH	Ni(I)−$(CD_3OH)_n$	2.323	2.131	2.068	F
H_2	ND_3	Ni(I)−$(ND_3)_n$	2.314	2.192	2.058	G
H_2	CO	Ni(I)-CO	2.253	2.192	2.064	H
C_2D_4/473 K		Ni(I)−$(C_2D_4)_n$	2.615	2.481	1.985	I
		Ni(I)−$(C_2D_4)_n$	2.718	2.356	1.971	J
C_2D_4/623 K		Ni(I)−$(C_4D_8)_n$	2.687	2.479	1.996	K
		Ni(I)−$(C_4D_8)_n$	2.272	2.181		L
NO/298 K		Ni(I)−$(NO)^+$	2.433	2.192		P
		Ni(I)−$(NO)^+$	2.368	2.161		O

Hydrogen reduction of NiNaK−Clino produces two different Ni(I) species (species C and D). These species are assigned to isolated Ni(I) ions in NiNaK−Clino, since they remain visible after evacuation at room temperature. The observation of two

species suggests that two isolated Ni(I) ions are located at different sites in the clinoptilolite structure.

When a hydrogen-reduced sample is kept at room temperature without outgassing of hydrogen, the intensities of species C and D decrease and a new species E is formed. This species can be assigned to a Ni(I)−$(H_2)_n$ complex on the basis of the following observations. First, species E does not appear when the sample is annealed at room temperature without hydrogen gas. Second, this species is stable at room temperature as long as hydrogen is kept inside the sample cell. Finally, Ni(I) easily decays at room temperature with the formation of Ni(II) and Ni(0). However, the ESR spectrum obtained after annealing a hydrogen-reduced sample with hydrogen shows no baseline-broadening caused by the formation of metallic nickel.

Adsorption of methanol on hydrogen-reduced NiNaK−Clino produces a single Ni(I)−$(CD_3OH)_n$ species, while species C assigned to an isolated Ni(I) remains unchanged. This indicates that species C is in a clinoptilolite site that is inaccessible to methanol. In contrast to methanol adsorption, both Ni(I) species C and D interact with ammonia to form a prominent Ni(I)−$(ND_3)_n$ species. We assume that Ni(I) species C is probably located at M3 sites at the center of channel C and is isolated from methanol molecules when the cations in M1 and M2 sites coordinate with methanol molecules. This assumption is based on the fact that cations in M1 and M2 sites move to a channel intersection upon dehydration and that the M1 and M2 sites are more accessible to adsorbates entering the two-dimensional channel system of clinoptilolite. Methanol molecule access to Ni(I) species C is then blocked by the cation−methanol complexes, since methanol is bigger than ammonia. This is supported by the observation that Ni(I) species C is not changed after a methanol-adsorbed sample is kept at room temperature for a longer time.

Thermal reduction is another reduction method used to produce paramagnetic Ni(I) ions in NiNaK−Clino. When a sample is dehydrated at 573 K for 12 h, a single Ni(I) species (species A) with rhombic symmetry is observed due to desorbing water and hydroxyl groups. This species is easily further reduced to metallic Ni(0) by increasing the temperature to 623 K. This indicates that a Ni(I) species formed by thermal reduction in clinoptilolite is not stable and is sensitive to the reduction temperature. The ESR parameters of this species A are also different from those of isolated Ni(I) species C and D observed after hydrogen reduction, showing a different environment for Ni(I) species A. This reduction behavior of NiNaK−Clino is unusual compared to other zeolites and SAPO materials. An isolated Ni(I) species was observed in Ni(II)-exchanged X, Y zeolites and SAPO materials during dehydration. This species was stable upon further heating to a higher temperature (873 K) and assigned to an isolated Ni(I) species, since the same species was produced by hydrogen reduction and this species remained unchanged upon evacuation. We can assume that Ni(I) species A obtained in NiNaK−Clino is due to an isolated Ni(I) ion or a Ni(I) complex with the remaining water molecules. Unfortunately, it is not possible to carry out ^{2}D ESEM measurement of species A, since the ESR signal of species A is so weak and is overlapped with a sharp radical signal.

Species H, a Ni(I)−carbonyl complex, is obtained after adsorption of CO on H_2-reduced NiNaK−Clino at room temperature. The observation that two Ni(I) species generated by hydrogen reduction disappear with the formation of one nickel−carbonyl complex (species H) indicates that both Ni(I) sites are accessible to carbon monoxide. Species H is also obtained after reduction of dehydrated Ni(II)NaK−Clino with CO at 623 K. The ESR spectrum with 90% ^{13}C-enriched ^{13}CO instead of ^{12}CO shows ^{13}C hyperfine structure, since ^{13}C has a nuclear spin of $^1/_2$. The doublet splitting of the g_3 component indicates one CO coordinating to Ni(I). On the basis of the observation that the use of higher CO pressure leads to the same ESR spectrum as that observed when low CO pressure is used, it is reasonable to assume that the maximum number of CO molecules coordinating to Ni(I) is one. The simulation of the ^{13}C ESEM spectrum also shows that a Ni(I) ion coordinates with one CO molecule at a distance of 0.33 nm.

The behavior of NiNaK−Clino upon CO adsorption is different from that observed in NiCa−X[18,25] and NiCa−Y zeolites.[26] The Ni(I) species, reduced by hydrogen in these materials, reversibly interacts with one to three CO molecules depending on the CO pressure and leads to the formation of Ni(I)−$(CO)_n$ complexes where the maximum number of CO molecules coordinated to Ni(I) is three. These different behaviors are attributed to a difference in the zeolite structures. X and Y zeolites are characterized by large 12-ring cages. Clinoptilolite contains no large cages, and its largest channel is a 10-membered ring.

Ethylene adsorption at room temperature on hydrogen-reduced NiNaK−Clino produces a broad signal due to Ni(0) superimposed with signals assigned to Ni(I) species C and D. This suggests that ethylene is not adsorbed on Ni(I) sites at room temperature as well as carbon monoxide is. However, when a dehydrated Ni(II)NaK−Clino sample is reduced by ethylene at the temperature above 373 K, species I and J assigned to Ni(I)−$(C_2D_4)_n$ complexes are easily generated. This suggests that Ni(II) in the channels of clinoptilolite can be reduced by ethylene and form a complex with ethylene at high temperature. These species are stable at room temperature as long as ethylene is not removed. The ESR spectra remain unchanged after prolonged heating at 473 and 573 K. However, when a sample is heated to 623 K for 30 min, species I and J almost disappear and a new species K with $g_1^K = 2.687$, $g_2^K = 2.479$, and $g_3^K = 1.996$ is observed. Species K is assigned to a Ni(I)−(C_4D_8) complex. Thus, ethylene dimerization occurs above 623 K in NiNaK−Clino. The ESEM data for species K confirm the formation of a Ni(I)−butene complex, indicating a σ-type interaction between Ni(I) ion and butene. This result confirms that Ni(I) ions formed by reduction with ethylene are active sites for ethylene dimerization.

The formation of Ni(I)−butene complexes was also observed as a result of ethylene dimerization in Ni(II)-exchanged SAPO-5 and SAPO-11.[22,27] These materials have 12-ring and 10-ring main channels, respectively. Intermediate Ni(I) ions are active sites for ethylene dimerization in both SAPO and NiNaK−Clino materials. The difference is in the reduction method to produce active Ni(I) sites. In SAPO materials, the Ni(I) is formed by hydrogen reduction and ethylene dimerization occurs at room temperature or 353 K. However, in clinoptilolite, Ni(I) sites are generated by direct reduction with ethylene and products of ethylene dimerization are obtained by controlling the temperature. This difference between NiNaK−Clino and SAPO materials for ethylene dimerization is attributed to different locations of the Ni(I) ions. In SAPO materials, Ni(I) is mostly located at the center of a hexagonal prism where an ethylene is too big to enter. On the other hand, Ni(I) and Ni(II) ions in clinoptilolite are located in channels where they are easily reduced by ethylene.

Nitric oxide adsorption on nickel-exchanged NiNaK−Clino produces two different paramagnetic species (species O and P)

along with a NO radical species (species Q). Ni(II) is reduced to Ni(I) by NO molecules, since the unpaired electron is easily transferred from NO molecule to the 3d orbitals of Ni(II), as its moderate ionization potential (9.5 eV) indicates.[28] Species with similar g values and line shapes have been reported in Ni−Y zeolite[28] and NiNa−A zeolite[29] and were assigned to Ni(I)−NO^+ complexes where the Ni(I) coordinates with three framework oxygens. In Ni−A zeolites, most of the Ni(I) ions are located in SI sites in hexagonal prisms and interact with one NO molecule to form two distinct Ni(I)−NO^+ complexes. Similarly, the observation of two species after NO adsorption on NiNaK−Clino suggests two Ni(I)−NO^+ complexes probably located near M2 sites where the nickel ions coordinate with three framework oxygens. The intensities of two Ni(I)−NO^+ species reflect the relative proportions of them.

Even though NO has an unpaired electron, it usually exhibits no paramagnetism in the ground state,[30] since the odd electron is localized in a degenerate π^* antibonding orbital. Therefore, no ESR signal is observed for gaseous NO molecules. However, the electric fields associated with the zeolitic cations can lift the degeneracy of the antibonding π^* orbitals and allow the odd electron to occupy a nondegenerate π^* orbital, making the ESR spectrum of this radical observable. In fact, the adsorption of NO on clinoptilolite shows an ESR signal due to NO radical whose π-orbital degeneracy has been lifted by the cations of clinoptilolite. When NO is adsorbed on NaK−Clino, the ESR spectrum shows hyperfine structure on the $g_\perp$ component of NO with $A_\perp^Q$ of 29 G. The splitting and the principal g values of this signal are very similar to those reported in Y zeolites containing different cocations such as Ba, Zn, and Na.[30]

Conclusions

ESR results have revealed that Ni(II) ions in NiNaK−Clino are reduced to Ni(I) by thermal and hydrogen reduction. Dehydration of NiNaK−Clino at 573 K produces a single Ni(I) species with rhombic symmetry. Hydrogen reduction produces two isolated Ni(I) ions that transform to a Ni(I)−$(H_2)_n$ complex after annealing at room temperature. Adsorption of methanol on reduced NiNaK−Clino forms a complex with one of the isolated Ni(I) ions, while the other isolated Ni(I) (species C) remains unaffected, indicating an inaccessible environment for this Ni(I). On the other hand, adsorption of ammonia forms complexes with both isolated Ni(I) ions. A prominent species is obtained by adsorption of CO on hydrogen-reduced NiNaK−Clino at room temperature or by direct reduction of dehydrated Ni(II)NaK−Clino with CO at 623 K. On the basis of isotope labeling and ^{13}C ESEM analysis, this species is identified as a Ni(I)−CO complex. Two Ni(I)−$(C_2D_4)_n$ species are observed after adsorption of ethylene on dehydrated Ni(II)NaK−Clino and subsequent heating below 623 K. At higher temperature, a Ni(I)−$(C_4D_8)_n$ complex is formed as a result of ethylene dimerization. Adsorption of NO on dehydrated Ni(II)NaK−Clino produces two Ni(I)−NO^+ complexes suggested to be located near M2 sites within the clinoptilolite structure.

Acknowledgment. This research was supported by the National Science Foundation and the Robert A. Welch Foundation. We thank Dr. D. Zhao for his help with the synthesis of clinoptilolite.

References and Notes

(1) Gottardi, G.; Galli, E. *Natural Zeolites*; Springer-Verlag: Berlin, 1985; p 256.
(2) Koyama, K.; Takeuchi, Y. *Z. Kristallogr*. **1997**, *145*, 216.
(3) Smyth, J. R.; Sapid, A. T. *Am. Mineral.* **1990**, *75*, 522.
(4) Vaughan, D. E. W. In *Natural Zeolites: Occurrence, Properties, Use*; Sand, L. B., Mumpton, F. A., Eds.; Pergamon: Oxford, 1978; pp 353−371.
(5) Shelef, M. *Chem. Rev*. **1995**, *95*, 209.
(6) Minachev, Kh. M.; Garanin, V. I.; Kharlamov, V. V.; Isakova, T. A. *Kinet. Catal.* **1972**, *13*, 1101.
(7) Ghosh, A. K.; Kevan, L. *J. Am. Chem. Soc*. **1988**, *110*, 8044.
(8) Biale, J. U.S. Patent 3 738 977, 1973.
(9) Williams, C. D. *J. Chem. Soc., Chem. Commun*. **1997**, 2113.
(10) Zhao, D.; Szostak, R.; Kevan, L. *Energy Lab. Newsl.* **1997**, *34*, 5.
(11) Kazansky, V. B.; Elev, I. V.; Shelimov, B. N. *J. Mol. Catal*. **1883**, *21*, 265.
(12) Ghosh, A K.; Kevan, L. *J. Phys. Chem.* **1990**, *94*, 3117.
(13) Kevan, L. In *Time Domain Electron Spin Resonance*; Kevan, L., Schwartz, R. N., Eds.; Wiley-Interscience: New York, 1979; Chapter 8.
(14) Azuma, N.; Kevan, L. *J. Phys. Chem.* **1995**, *99*, 5083.
(15) Prakash, A. M.; Wasowicz, T.; Kevan, L. *J. Phys. Chem.* **1996**, *100*, 15947.
(16) Azuma, N.; Hartmann, M.; Kevan, L. *J. Phys. Chem.* **1995**, *99*, 6670.
(17) Prakash, A. M.; Hartmann, M.; Kevan, L. *J. Chem. Soc., Faraday Trans.* **1997**, *93*, 1233.
(18) Kermarec, M.; Oliver, D.; Richard, M.; Chen, M. *J. Phys. Chem.* **1982**, *86*, 2818.
(19) Schoonheydt, R. A.; Roodhooft, D. *J. Phys. Chem.* **1986**, *90*, 6319.
(20) Michalik, J.; Narayana, M.; Kevan, L. *J. Phys. Chem.* **1984**, *88*, 5236.
(21) Hartmann, M.; Azuma, N.; Kevan, L. *J. Phys. Chem.* **1995**, *99*, 10988.
(22) Hartmann, M.; Kevan, L. In *Progress in Zeolite and Microporous Materials*; Chon, H., Ihm, S. K., Uh, Y. S., Eds.; Studies in Surface Science and Catalysis 105A; Elsevier: Amsterdam, 1997; p 717.
(23) Ackley, M. W.; Giese, R. F.; Yang, R. T. *Zeolites* **1992**, *12*, 780.
(24) Armbruster, T. *Am. Mineral.* **1993**, *78*, 260.
(25) Oliver, D.; Richard, M.; Che, M. *Chem. Phys. Lett*. **1978**, *60*, 77.
(26) Garbowski, E.; Vedrine, J. *Chem. Phys. Lett*. **1977**, *48*, 550.
(27) Hartmann, M.; Kevan, L. *J. Chem. Soc., Faraday Trans*. **1996**, *92*, 1429.
(28) Naccache, C.; Taarit, Y. *J. Chem. Soc., Faraday Trans.* **1973**, *69*, 1475.
(29) Hennebert, P.; Hemidy, J.; Cornet, D. *J. Chem. Soc., Faraday Trans.* **1980**, *76*, 952.
(30) Kasai, P. K.; Bishop, R. J. *J. Am. Chem. Soc*. **1972**, *94*, 5560.